Ion–ionophore interactions in polymeric membranes studied by thin layer voltammetry

Mao, Canwei; Robinson, Kye; Yuan, Dajing; Bakker, Eric

How to cite

MAO, Canwei et al. Ion–ionophore interactions in polymeric membranes studied by thin layer voltammetry. In: Sensors and actuators. B, Chemical, 2022, vol. 358, p. 131428. doi: 10.1016/j.snb.2022.131428

This publication URL: https://archive-ouverte.unige.ch/unige:164196
Publication DOI: 10.1016/j.snb.2022.131428

Sensors & Actuators: B. Chemical 358 (2022) 131428

Contents lists available at ScienceDirect

Sensors and Actuators: B. Chemical

journal homepage: www.elsevier.com/locate/snb

Ion–ionophore interactions in polymeric membranes studied by thin layer voltammetry

Canwei Mao [a], Kye J. Robinson [a], Dajing Yuan [b,*], Eric Bakker [a,*]

[a] Department of Inorganic and Analytical Chemistry, University of Geneva, Quai Ernest-Ansermet 30, CH-1211 Geneva, Switzerland
[b] Anhui Key Laboratory of Chemo-Biosensing, College of Chemistry and Materials Science, Anhui Normal University, Wuhu 241000, PR China

ARTICLE INFO

Keywords:
Complex formation constant
Stoichiometry
Selectivity coefficient
Ion-ionophore interaction
Ion-surfactant interaction

ABSTRACT

In ion sensing applications, selective ion-receptor complexation is the molecular basis for endowing the sensing material with selectivity. In this work, thin polymeric membrane-based ion transfer voltammetry is used to investigate ion-receptor complexation, using a range of electrically neutral ionophores and surfactants as examples. Previous studies lacked a convincing approach to eliminate the influence from transducing layer, resulting in deviations of the observed binding constants compared to potentiometric methods. A recently developed method allows for subtracting the potential changes of the transducing layer, thereby overcoming this challenge. Using this approach, a range of ionophores are assessed. Valinomycin for the detection of potassium gave a logarithmic complex formation constant in the membrane of 9.69 ± 0.25 with a 1:1 stoichiometry. Lithium ionophore VI for lithium gave a logarithmic stability constant of 5.97 ± 0.06 with 1:2 complexes; while sodium ionophore X for sodium (7.57 ± 0.03, 1:1) and calcium ionophore IV for calcium (21.57 ± 0.25, 1:3) were also characterized, in addition to their complexes with potential interfering ions. The complex formation of three surfactants with potassium are also explored in membranes containing valinomycin, with Brij-35 (4.88 ± 0.08, 1:1), Triton X-100 (5.63 ± 0.10, 1:1), F-127 (4.63 ± 0.49, 1:1). Limitations of the approach are discussed, which includes the need for electrochemical reversibility and a sufficiently high lipophilicity to adequately retain the components in the membrane

1. Introduction

Polymeric ion-selective membranes (ISMs) used in potentiometric sensing probes are based on a matrix normally composed of polymer and plasticizer, lipophilic ion exchanger and selective ion receptor (ionophore) [1]. Ionophore-free membranes always show the same selectivity pattern in the order of the hydration energy of the ions of interest. Distinctly different selectivity may be observed in the presence of a lipophilic molecular receptor (ionophore and surfactant), driven by the complex formation constants between the extracted ion and the receptor [2,3]. Ion-receptor complexation constants often dramatically differ from those observed in bulk solution as obtained spectroscopically (NMR titrations) owing to the specific solvent environment of ion-selective membranes [4,5].

The optimum molar ratio of ionophore to ion exchanger in the membrane depends on the complex stoichiometries, in which case the influence of the ion-exchanger concentration can be very large [6]. Some ionophores also may form mixed complexes [7] and the optimal ratio will depend on the relative strength of the resulting forms [8,9]. When multiple complex stoichiometries are simultaneously relevant in the membrane, the optimal ionophore to ion-exchanger ratio cannot easily be predicted theoretically and needs to be found by experiment [7].

A limited number of experimental techniques are available to assess ion-ionophore complex formation constants directly in the membrane [10–12], of which the potentiometric sandwich membrane approach is perhaps the most widely used [11]. The principle of the approach rests on the effective uncoupling of both phase boundary potentials by imposing a well-defined initial ion concentration profile in the membrane [13]. This method can be sufficiently precise and accurate, but it provides just a single data point per experiment that reflects the chosen membrane composition. Membranes have also started to be characterized by dynamic electrochemistry, for example by ion transfer voltammetry [14,15] or by controlling the current (pulstrodes) to achieve instrumentally tunable selectivity [16]. These approaches, however, tend to be less robust than potentiometric methods because the current

* Corresponding authors.
E-mail addresses: dajing.yuan@ahnu.edu.cn (D. Yuan), eric.bakker@unige.ch (E. Bakker).

https://doi.org/10.1016/j.snb.2022.131428
Received 30 November 2021; Received in revised form 9 January 2022; Accepted 14 January 2022
Available online 29 January 2022

is typically either limited by mass transport kinetics in solution or in the membrane.

In recent years, relatively thin ion-selective membranes on the order of one micrometer or less and backside contacted with a conducting polymer have been described and theoretically modeled [12,17,18]. Under optimal experimental conditions, the influence of mass transport on the current response can be eliminated, and thus this system can characterize ion–ionophore interactions in ion-selective membranes under conditions that approach equilibrium [12,19]. The interaction in this system corresponds to an electrochemical dosing of ionic reagents, which is more attractive than potentiometric methods. However, a major drawback is that such thin film-based membranes must have backside contact with a transducing layer material that exhibits its own electrochemical characteristics, with a potential that is not easily described as a function of applied charge. Earlier work assumed a linear relationship between charge and potential change for the conducting polymer layer to study ion-ionophore interactions, resulting however in larger complex formation constants than those obtained by potentiometric methods [12]. Recently, we introduced an improved approach to separate the potential change of the inner transducing layer during a linear potential scan by using the ion transfer of a lipophilic reference ion [20]. The current response is then integrated and expressed as available ion-exchanger concentration, so that the voltammogram is converted to a titration curve for the membrane. Here we apply this method beyond the early example given in [17] to investigate several ionophores and non-ionic surfactants for their complex formation constant and binding stoichiometry.

2. Theory

The voltammetric ion transfer process is shown in Scheme 1 with the conducting polymer poly(3-octyl thiophene) (POT) as a model transducing material that may be substituted for another suitable material as needed. A linear potential scan gradually converts the transducer polymer, POT, to its oxidized form, POT^+. This depletes cation-exchanger, R^-, from the thin membrane layer to maintain electroneutrality. As a result, the cation M is transferred from the membrane phase to the aqueous phase. The membrane contains excess ion-exchanger over ionophore so that the transfer of ionophore-bound and free ion (M) can both be observed in a single scan. If a surfactant is additionally involved in the ion transfer process, the ion-surfactant complex formation constant can simply be calculated using the potential difference between the ion-ionophore complex peak and that corresponding to surfactant. Ion transfer is limited by the available ion-exchanger because the transducing material is used in excess and as such has a larger redox capacity.

The change in applied potential $E_M(t)$ is understood to originate from the sum of two phase boundary potentials. One is for the transfer of the ion M at the solution–membrane interface, $\Delta^m_{aq}\phi_M(t)$. The other is for the redox reaction of the POT transducing layer, $\Delta\phi_{POT}(t)$, shown as

$$E_M(t) = \Delta\phi_{POT}(t) + \Delta^m_{aq}\phi_M(t) \quad (1)$$

As described earlier [20], the ion-selective membrane is first interrogated in a solution containing a salt of just TBA, baseline corrected and expressed as a function of passed charge by integrating the current over time. This charge is then translated into available ion-exchanger concentration by considering that the ion-exchanger is the limiting reagent. The calculated value for the transfer potential of the reference ion TBA (eq S5) is then subtracted from the experimental function of potential vs. ion-exchanger concentration, giving the isolated potential for the inner membrane side in contact with the transducing layer (e.g., POT):

$$\Delta\phi_{POT}(c_R) = E_{TBA}(c_R) - \Delta^m_{aq}\phi_{TBA}(c_R) \quad (2)$$

where $E_{TBA}(c_R)$ is the applied potential in solution containing TBA and $\Delta^m_{aq}\phi_{TBA}(c_R)$ is the calculated TBA ion transfer potential at the solution–membrane interface as a function of available ion-exchanger concentration, c_R. Note that in this treatment ion activities in the membrane phase are replaced by concentrations for simplifying the calculations involving mass and charge balances. The desired potential for the ion transfer of *M*, $\Delta^m_{aq}\phi_M$, may now be obtained by subtracting $\Delta\phi_{POT}$ (Eq. 2) from the experimental potential, $E_M$for each value of c_R:

$$\Delta^m_{aq}\phi_M(c_R) = E_M(c_R) - \Delta\phi_{POT}(c_R) \quad (3)$$

This experiment is performed on the same membrane as for the experiment with TBA. The potential change as a function of available ion-exchanger concentration may be used to find the relevant binding constants and complex stoichiometries by curve fitting. The function is described as following for membranes containing an electrically neutral ionophore and a total ion-exchanger concentration in molar excess. The mass balance for the ionophore, charge balance and complex formation constant are given by Eqs. (4)–(6), respectively,

$$L_T = c_L + \sum_n n c_{ML_n} \quad (4)$$

$$\beta_{ML_n} = \frac{c_{ML_n}}{c^m_M (c_L)^n} \quad (5)$$

$$c_R = z_M \left(c^m_M + \sum_n c_{ML_n} \right) \quad (6)$$

where L_T is the total concentration of electrically neutral ionophore in the membrane, $c_{ML_n}$the concentration of all complexes ML_n (with a 1:n stoichiometry between *M* of charge z_M and the ionophore), c_L the

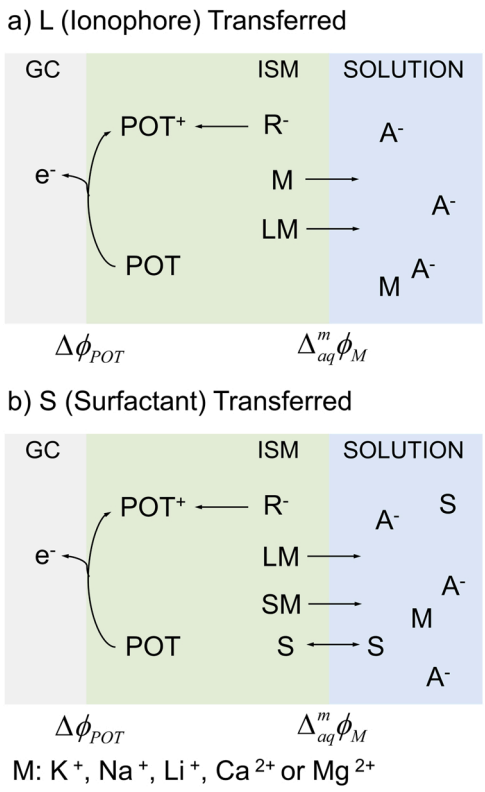

Scheme 1. Working mechanism of thin polymeric membrane for a linear oxidation potential scan with different receptors-assisted ion transfer a) membrane doped with ionophore b) membrane with surfactant partition from bulk solution containing analyte ions, M. GC = Glassy Carbon; ISM = Ion Selective Membrane; POT = poly(3-octylthiophene); R^- = lipophilic cation exchanger; L = Ionophore; S = Surfactant; A^- = Anion. $\Delta\phi_{POT}$ is the potential for POT oxidation; $\Delta^m_{aq}\phi_M$ is the Galvani potential differences for the transfer of M between the membrane and solution interface.

concentration of uncomplexed ionophore in the membrane, and β_{ML_n} the overall complex formation constant. Phase labels (m for the membrane and aq for the aqueous phase) are only given for the species that may be present in the aqueous and membrane phase, such as the ion M^{z+}. For a monovalent ion (z_M=1) forming complexes of a 1:1 complex stoichiometry (n = 1), the available ion-exchanger concentration c_R (which is described by the charge passed) can be expressed as a function of c_M^m by combining Eqs. (4)–(6) to eliminate c_L and c_{ML_n}:

$$c_R = \frac{c_M^m\left(1 + c_M^m\beta_{ML} + \beta_{ML}L_T\right)}{1 + c_M^m\beta_{ML}} \tag{7}$$

The membrane concentration of the so-called free ion M, c_M^m, is a function of the ion transfer potential (see also eq S4):

$$c_M^m = c_M^{aq}10^{-\left(\Delta_{aq}^m\phi_M - \Delta_{aq}^m\phi_M^0\right)/s} \tag{8}$$

where s is the Nernstian slope. Hence, the relationship between potential change and c_R can be obtained from Eqs. (7) and (8).

Using the same type of assisted ion transfer process, the behavior for a membrane containing electrically neutral surfactants partitioning from aqueous solution may be described. For this, Eqs. (5) and (6) are adapted by describing the partition coefficient p_S of the surfactant S between solution and membrane,

$$p_S = \frac{c_S^m}{c_S^{aq}} \tag{9}$$

and the complex formation constant between surfactant and M^{z+} in the membrane

$$\beta_{MS_q} = \frac{c_{MS_q}^m}{c_M^m\left(c_S^m\right)^q} \tag{10}$$

$$c_R = c_M^m + c_{ML_n} + c_{MS_q} \tag{11}$$

where c_S^m and c_{MS}^m are the membrane concentrations of uncomplexed and complexed surfactant, respectively. If the surfactant forms 1:1 complexes only (q=1), the equations may be further simplified as follows. Solving Eqs. (4), (5), (9), (10) and (11) (adapting surfactant complex in the charge balance) gives a function of ion concentration in the membrane as a function of available ion-concentration and hence of potential,

$$c_R = \frac{c_M^m\left(1 + c_M^m\beta_{ML} + L_T\beta_{ML} + p_Sc_S^{aq}\beta_{MS} + c_M^mp_Sc_S^{aq}\beta_{ML}\beta_{MS}\right)}{1 + c_M^m\beta_{ML}} \tag{12}$$

Eq. (8) may again be used with Eq. (12) to describe the relationship between c_R and the ion transfer potential. Other cases for different ion valency and different complex stoichiometry are given in Eqs S6-S12 in SI.

3. Experimental

3.1. Reagents, materials and equipment

Aqueous solutions were prepared by dissolving the appropriate salts in deionized water (ca. 18 MΩ cm). Lithium perchlorate ($LiClO_4$, >98%,), 3-octylthiophene (97%, OT), potassium chloride (KCl, ≥99.5%), sodium chloride (NaCl, ≥99.5%), lithium chloride (LiCl, ≥99.0%), calcium chloride ($CaCl_2$, ≥96%), magnesium chloride ($MgCl_2$, ≥97%), tetrabutylammonium chloride (TBACl), high molecular weight poly(vinyl-chloride) (PVC), polyurethane pellets (PU, Selectophore™), bis(2-ethylhexyl)sebacate (DOS), sodium tetrakis[3,5-bis-(trifluoromethyl)phenyl]borate (NaTFPB), potassium ionophore I (Valinomycin, K-I), 4-tert-Butylcalix [4] arene-tetraacetic acid tetraethyl ester (Na ionophore X, Na-X), 6,6-Dibenzyl-1,4,8–11-tetraoxacyclotetradecane, 6,6-Dibenzyl-14-crown-4 (Li ionophore VI, Li-VI), Brij®35 (Brij-35), Pluronic® F-127 (F127), Triton™ X-100 (TX-100), acetonitrile (ACN) and tetrahydrofuran (>99.9%, THF) were purchased from Sigma Aldrich. N,N-Dicyclohexyl-N′,N′-dioctadecyl-3-oxapentanediamide, N,N-Dicyclohexyl-N′,N′-dioctadecyl-diglycolic diamide (ETH 5234, Ca-IV) was purchased from Fluka Analytical. The structures of the ionophores studied here are shown in Scheme 2.

GC-electrode with diameter of 3.00 ± 0.05 mm was sourced from Metrohm (Switzerland). Cyclic voltammograms were recorded with a PGSTAT 101 (Metrohm Autolab B.V., Utrecht, The Netherlands) controlled by Nova 2.1 software (supplied by Autolab) running on a PC. A double-junction Ag/ AgCl/3 M KCl/1 M LiOAc reference electrode (6.0726.100 model, Metrohm, Switzerland) and a platinum electrode as counter electrode (6.0331.010 model, Metrohm, Switzerland) were used in a three-electrode cell. A LabSpin instrument (from SUSS MicroTec) was used to spin coat the thin membranes on the POT modified electrodes at 1500 rpm. A 16-channel EMF interface (Lawson Laboratories, Inc., Malvern, PA) was used for potentiometric measurements. Wolfram Mathematica® 12 software was used to develop the theory and the final data fit.

3.2. Preparation of the electrodes

Poly(3-octylthiophene) (POT) was electrochemically polymerized on glassy carbon electrode (GC) surface by cyclic voltammetry (two scans, 0–1.5 V, 100 mV s^{-1}). A solution containing 0.1 M 3-octylthiophene and 0.1 M $LiClO_4$ in acetonitrile was used. The POT underlayer was then coated with 25 μL of the diluted membrane cocktail (dilution of 1:4 in THF) by spin-coating at 1500 rpm for 2 min until the THF completely evaporated, to obtain the thin film ISM electrode. Table S1 shows the compositions of the membrane cocktails (referred to a total weight of 100 mg) prepared in 1 mL THF.

3.3. Electrochemical experiments

Each ISM GC electrode containing an excess amount of ion exchanger over ionophore was used to measure the primary ions following interfering ions with cyclic voltammetry in the range between − 0.4 V and 1.5 V with a scan rate of 0.1 V/s (unless otherwise indicated) before

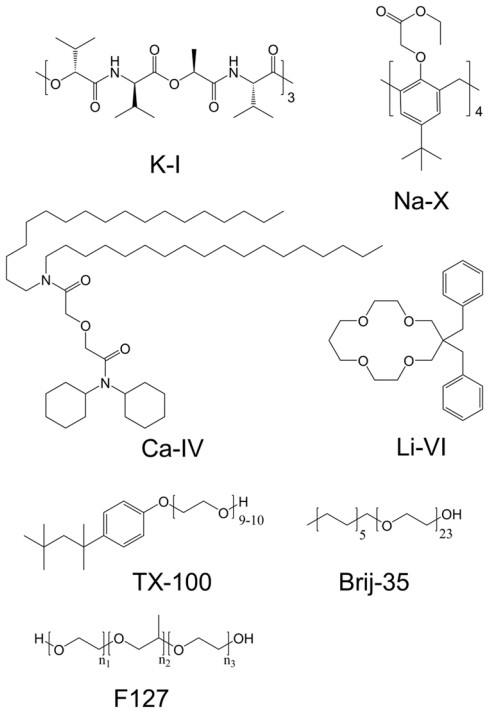

Scheme 2. Chemical structures of the receptors studied in this work.

measuring TBA^+. The measurement sequence for each interfering ion followed the Hofmeister sequence (e.g. $MgCl_2$, LiCl, NaCl, KCl, $CaCl_2$ and then TBACl for calcium-selective electrode), which helps to avoid the interference of each analyte and obtain unbiased selectivity coefficients [21]. In between changing each solution, the ISE was dipped in clean DI water as a gentle rinse and the component leakage was interrogated, shown in Fig. S3c. The concentration of each ion solution (KCl, NaCl, LiCl, $CaCl_2$, $MgCl_2$ and TBACl) was 10 mM. The standard deviation in the paper is based on three replicate experiments of three different membranes. More details are found in SI, Experimental Procedures.

4. Results and discussion

4.1. Boundary potential isolation

Two electrodes with electrochemically deposited POT as ion-to-electron transducing layer were produced and spin-coated with two different membranes, one with and one without the ionophore valinomycin (membranes MI and MII, see Table 1 for compositions), Fig. S1a. As our previous study also suggests that no interaction between TBA^+ and POT [20] was observed, we also show no interaction between TBA^+ and ionophore (Valinomycin as the typical model), thus the developed theory can be applied. TBA^+ has also been used in earlier studies as reference ion in potentiometric studies for ionophore steric hinderance and the lack of interaction was confirmed with sandwich membrane experiments [11]. To clarify, these reactions are schematically shown in Scheme 1. The exhaustive nature of this process explains the bell-shaped curve of the voltammogram. In the case of ionophore-assisted transfer, the observed peak is shifted to a more positive potential (like Fig. S1b). It is this shift that forms the basis of the method discussed here and the theory is established by Liu et.al. [17].

The approach is experimentally illustrated for TBA^+ in Fig. 1, which represents the baseline corrected anodic linear scan for TBA^+ that describes the electrochemical turnover as a function of applied potential. The baseline correction is performed with a first order polynomial baseline function within a potential range of about 1.2 V. The data shown in Fig. S1b is with the same membrane but for a solution containing K^+, as in previous work [20]. The data is then used with the same data postprocessing treatment to separate the POT boundary potential changes (see Fig. S2) [20].

In earlier work, POT oxidation kinetics was found to be negligible with surface confined experiments on the basis of the observed linear dependence of peak current on the scan rate [12]. This was here confirmed with a membrane containing only cation exchanger in 10 mM KCl at different scan rates (Fig. S3a). All anodic peaks gave the same relative charge as a function of potential with negligible deviation (Fig. S3b). This suggests that a sufficiently rapid electrochemical conversion to allow for an equilibrium treatment.

By processing the data from Fig. S1b as reported previously [20] the boundary potential changes of the POT and ion transfer can be obtained (dashed line in Fig. 2b) from integrating the current (Fig. 2a). As illustrated in Scheme 1, this membrane composition is chosen to result in two distinct ion transfer waves. A decrease of available cation-exchanger concentration upon oxidation of the ion-to-electron transducer first expels the potassium ion from the membrane as an uncomplexed ion and only subsequently from dissociating the valinomycin complex. The baseline corrected peaks (Fig. 1) for K^+ exhibit an integrated charge that is similar to the one for TBA^+ (for the two peaks of K^+: 4.99 μC, for the single peak of TBA^+: 5.06 μC). This is expected if the cation-exchanger is the limiting reagent in both cases. One may now subtract the potential change of POT as a function of charge from the experimental cell potential to obtain the isolated potassium transfer potential shown as blue dots in Fig. 2b.

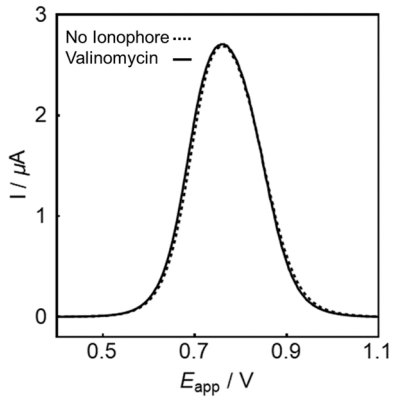

Fig. 1. Baseline corrected anodic scans for a membrane with and without ionophore valinomycin for the TBA^+ (10 mM TBACl in solution, the whole CV shown as Fig. S1a).

By doing so one arrives at the isolated potential change arising from the sample–membrane phase boundary. The discrete nature of this trace originates from sub-sampling because the subtracted potentials in the two data sets are not exactly the same, for example their potential window difference and baseline correction variation. The initial sharp decrease of the phase boundary potential at very low ion-exchanger concentrations visible in Fig. 2b is thought to originate from small variations of the cation-exchanger concentration between the different samples. It is considered an artifact that should not be taken into account for the extraction of binding constant data. A similar behavior is found for the theoretical fitting with the POT-subtracted data in Fig. 4b, 4d and 4f at lower potentials.

4.2. Theoretical study of the interaction between ionophores and different ions

4.2.1. The model ionophore K-I (Valinomycin)

The same membrane was tested in solution with different ions as mentioned above in the specified order, and it was gently dipped in pure DI water to rinse off the former residue solution on the electrode then placed into the next analyte solution. The leakage of the membrane components corresponding to the total charge integration of the peak area was evaluated from the change in total charge passed from the time integration of the current (see Fig. S3c). A slight decrease of the ion-exchanger concentration (c_R) was observed and corrected accordingly while fitting the theoretical model curve. The data are presented in analogy to a titration curve in which a potassium salt is consecutively added to a membrane containing valinomycin, with the resulting change in phase boundary potential as readout. Once potassium is in excess of valinomycin, the potential decreases drastically in agreement with eq S4 because it corresponds to an increase of the uncomplexed potassium concentration.

Quantitative data are extracted by fitting with equilibrium theory of

Table 1
Formation constants of four ionophores (K-I, Na-X, Li-VI and Ca-IV) towards different ions.

$\log\beta_{ILn}$	K-I	Na-X	Li-VI	Ca-IV
KL_1	**9.69 ± 0.25**	4.32 ± 0.03	2.48 ± 0.03	3.97 ± 0.06
NaL_1	5.10 ± 0.22	**7.57 ± 0.03**	–	4.84 ± 0.05
NaL_2	–	–	4.57 ± 0.21	–
LiL_1	3.59 ± 0.09	3.59 ± 0.09	–	4.27 ± 0.06
LiL_2	–	–	**5.97 ± 0.06**	–
CaL_1	5.83 ± 0.21	0.89 ± 0.10	0.47 ± 0.03	–
CaL_3	–	–	–	**21.57 ± 0.25**
MgL_1	5.62 ± 0.16	–	–	5.53 ± 0.05
MgL_3	–	8.70 ± 0.36	8.08 ± 0.03	12.23 ± 0.75

Note: n indicates the IL_n complex stoichiometry. The formation constant for the primary ion is in bold.

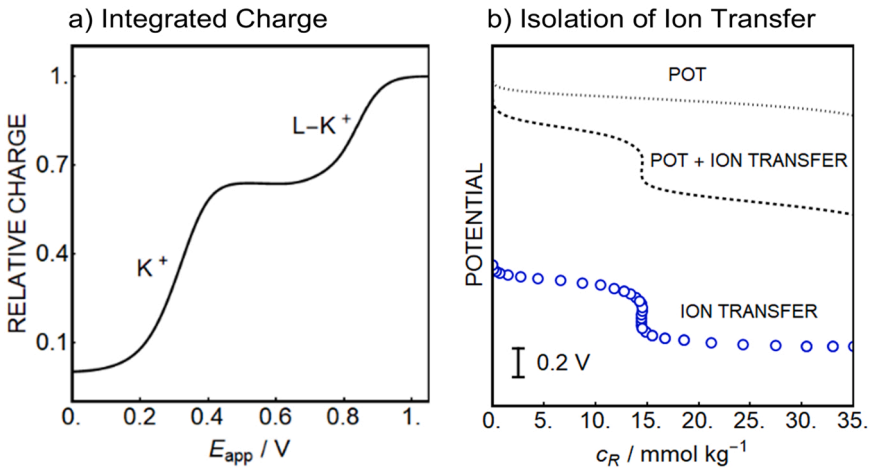

Fig. 2. a) Plot of integrated relative charge as a function of applied potential for K^+ in Fig. S1b. b) Plot of isolated potential for POT oxidation (top dotted trace), experimental applied potential (middle dashed trace, POT + ion transfer) and isolated galvanic potential difference (bottom blue dotted trace) as a function of cation exchanger in the membrane. (For interpretation of the references to colour in this figure legend, the reader is referred to the web version of this article.)

the type shown in Eqs. 7 and 8. For valinomycin, the model assumes a 1:1 complex stoichiometry for the potassium, sodium, lithium, calcium and magnesium complexes, as well as appropriate mass and charge balances for the membrane phase. The best fit from five replicates (separate membranes) gives log $\beta_{KL} = 9.59 \pm 0.20$, shown in Fig. 3a as solid trace together with the isolated phase boundary potential data (blue dots). The same procedure was also applied to a sample containing 10 mM NaCl for the same membrane (see Fig. S4a in Supplementary Data), with the appropriate traces and data points shown in Fig. 3a (red dots). The associated stability constant for the sodium complex was found to be $\log\beta_{NaL} = 5.10 \pm 0.22$. The values found for the complex formation constants for potassium and sodium in thin membranes compare favorably to those previously reported using sandwich membranes, $\log\beta_{KL} = 9.86 \pm 0.08$ and $\log\beta_{NaL} = 5.36 \pm 0.08$ respectively [13,22]. The formation constant for lithium is found in the same way (Fig. S4b), giving $\log\beta_{LiL} = 3.59 \pm 0.09$ as shown by the green dotted trace in Fig. 3a. The potential difference observed for potassium is larger than for sodium because of even greater binding strength. The experimental data for the binding of magnesium and calcium to valinomycin behave differently because of the divalent charge of the two ions (data

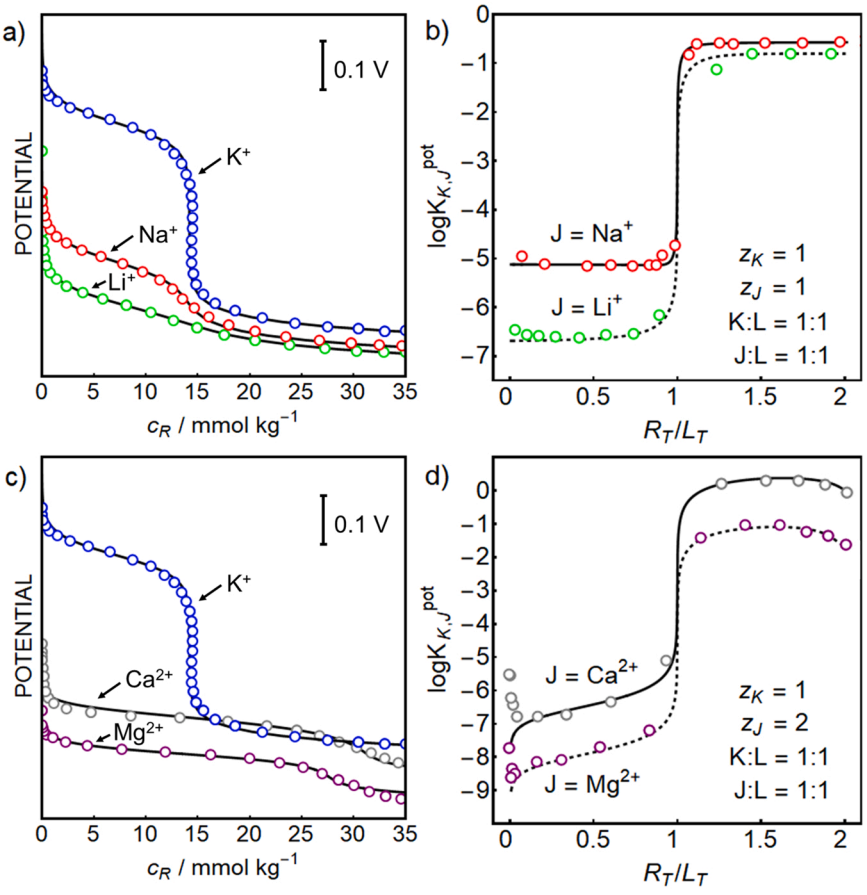

Fig. 3. a) and c) Theoretical fitting of ion transfer curves for potassium (blue trace, the same data as Fig. c, sodium (red trace), lithium (green trace), calcium (gray trace) and magnesium (purple trace) using equilibrium theory. The solid lines are calculated ones and the circle dotted traces are experimental ones; b) and d) The relationship of selectivity coefficient and ion exchanger to ionophore ratio. ($J = Na^+$ or Li^+ and Ca^{2+} or Mg^{2+}, z means the charge of the ion and the ratio associates to the stoichiometry), the color dots represent the selectivity coefficient of potassium over the corresponding ion from the experimental data from Fig. 3a and Fig. 3c. The solid and dashed lines correspond to the calculated curves from Fig. a and c as well. L means valinomycin. (For interpretation of the references to colour in this figure legend, the reader is referred to the web version of this article.)

postprocessing steps are shown in Fig. S4c and S4d). The results are shown in Fig. 3c, giving $\log\beta_{CaL} = 5.83 \pm 0.21$ and $\log\beta_{MgL} = 5.62 \pm 0.16$. While the formation constants are significant, the divalent charge means that these values reflect a weak stabilization. This is displayed by the small potential decrease at approximately twice the concentration of ion-exchanger, which indicates the point of saturation of valinomycin by the divalent ion.

In the cases described above, the potential differences between potassium and other ion potential traces provide a direct insight into membrane selectivity as a function of ion-exchanger concentration (Fig. 3b and d). At concentrations of ion exchanger higher than that of valinomycin, the modest observed selectivity for potassium reflects its smaller hydration energy (Hofmeister sequence). A logarithmic selectivity coefficient over sodium of -0.57 ± 0.01 and over lithium of -0.84 ± 0.16 is observed, explained by the lower lipophilicity of lithium than sodium. The best selectivity is found for $R_T < L_T$ for both cases of sodium and lithium, with a corresponding value of -4.92 ± 0.28 and -6.92 ± 0.32 respectively. These values follow a similar trend to literature values obtained using a conventional composition for potassium ion selective membranes $\log K_{K,Na}^{pot} = -4.5 \pm 0.1$ [21] and $\log K_{K,Li}^{pot} = -5.0$ [22]. The logarithmic selectivity coefficients measured here are somewhat larger, likely because thin membrane films exhibit fewer memory effects from residual potassium remaining in the membrane that can otherwise bias selectivity measurements [23]. While theory predicts that the optimal selectivity over lithium is at a low concentration of ion-exchanger (line in Fig. 3b)

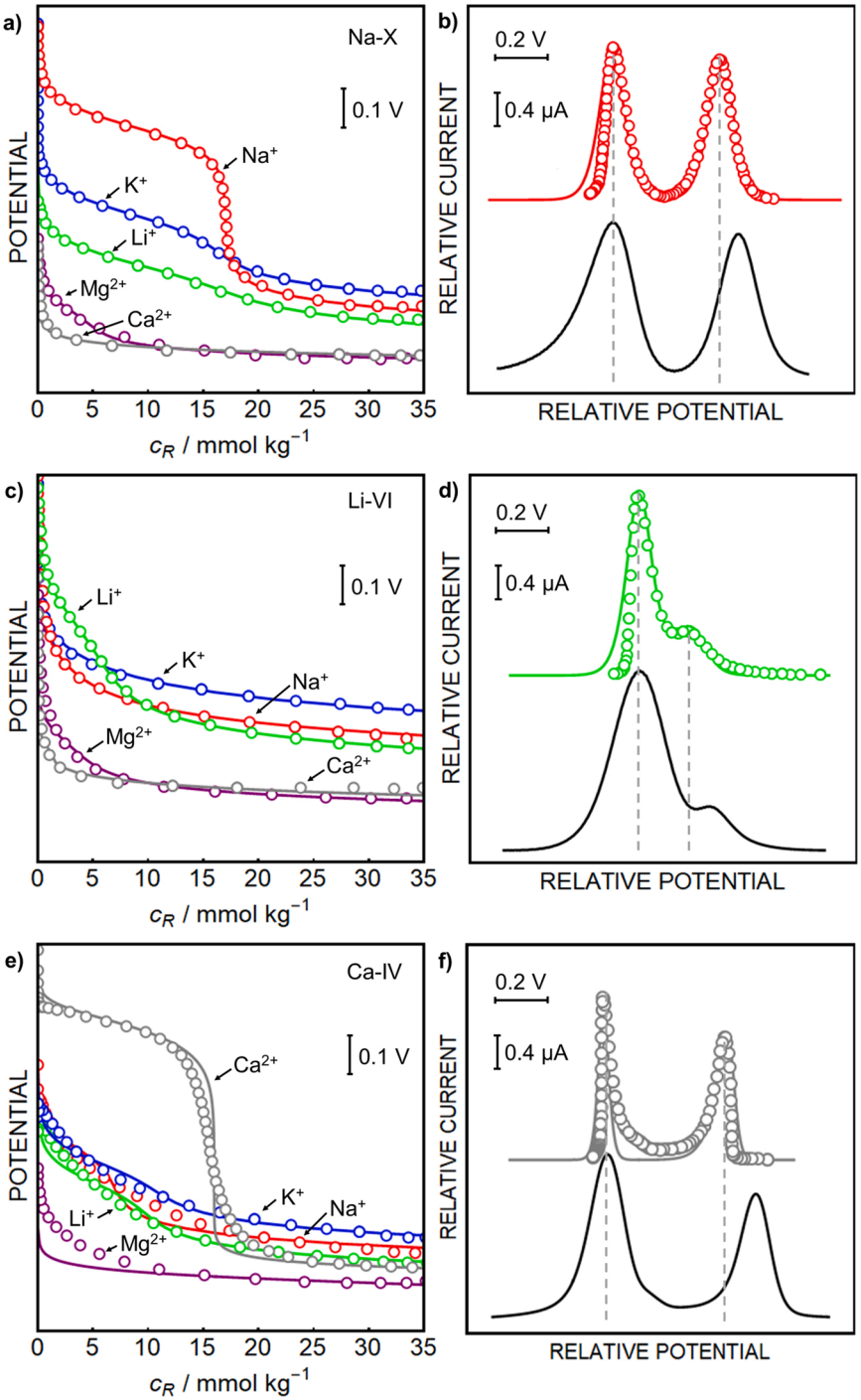

Fig. 4. Theoretical fitting of ion transfer curves for different ions using equilibrium theory with different stoichiometries and comparison with the experimental data, a) Na-X, c) Li-VI and e) Ca-IV performed in five different separated solutions, respectively. b), d) and f) are the primary ion transfer of each ionophore converted to current wave fitting with the theory comparing experimental data. The colors indicate the corresponding analyzed ions, blue: potassium, red: sodium, green: lithium, purple: magnesium and gray: calcium. (For interpretation of the references to colour in this figure legend, the reader is referred to the web version of this article.)

because of the weak binding, the experimental data suggest best selectivity at about 50% ion-exchanger relative to ionophore. For sodium, binding is more substantial and the selectivity is constant up to the point of valinomycin saturation, see also Fig. 3b.

The situation is different when valinomycin interacts with the divalent calcium or magnesium ions (Fig. 3d). Because the charges of the primary and interfering ions are not the same, the selectivity coefficient is different for each ion-exchanger concentration. Optimum selectivity is expected at minimal ion-exchanger concentration, which agrees with the experimental data. The selectivity coefficients for potassium over magnesium and calcium are found as $\log K_{K,Mg}^{pot} = -7.38 \pm 0.68$ and $\log K_{K,Ca}^{pot} = -6.63 \pm 0.37$ at $R_T / L_T = 0.5$, which agree well with literature values using a similar membrane composition, -7.5 ± 0.1 and -6.9 ± 0.1 [21], respectively.

4.2.2. The model ionophore Na-X

Fig. 4 summarizes the results for the other three ionophore studied in this work. Na-X exhibits selectivity to sodium because of its basket shaped cavity for sodium that forms a stable 1:1 complex [24,25]. The best fit from three replicates for Na-X with an assumed ion-ionophore complex stoichiometry of 1:1 gives $\log \beta_{NaL} = 7.57 \pm 0.03$ (Table 1). This value agrees well with the literature, $\beta_{NaL} = 7.69 \pm 0.05$ [22]. As Fig. 4a shows, Na-X gives a selectivity behavior most analogous to K-I. It is highly selective to sodium and forms a 1:1 complex. This stoichiometry is also obtained from fitting, giving the following complex formation constants: $\log \beta_{KL} = 4.23 \pm 0.03$, $\log \beta_{LiL} = 3.59 \pm 0.09$ and $\log \beta_{CaL} = 0.89 \pm 0.10$. Somewhat surprisingly the data suggest a 1:3 complex with magnesium, with $\log \beta_{MgL3} = 8.70 \pm 0.36$. By observing the potential difference between two ions for each ion-exchanger concentration, we obtain the selectivity coefficients at $R_T / L_T = 0.25$ as follows: $\log K_{Na,K}^{pot} = -2.73 \pm 0.07$, $\log K_{Na,Li}^{pot} = -4.33 \pm 0.07$, $\log K_{Na,Mg}^{pot} = -6.34 \pm 0.16$ and $\log K_{Na,Ca}^{pot} = -7.25 \pm 0.03$. These are comparable to the respective experimental selectivity coefficients reported in the literature of $\log K_{Na,K}^{pot} < -2.5$, $\log K_{Na,Li}^{pot} < -3.8$, $\log K_{Na,Ca}^{pot} < -3.9$, $\log K_{Na,Mg}^{pot} < -4.1$ [26,27]. Fig. 4b shows how the experimental sodium transfer wave varies before and after POT subtraction. Clearly, the separation of the two peaks for the transfer with and without ionophore become smaller upon isolation of the wave (top trace) relative to the uncorrected data (bottom black trace). Moreover, the ion transfer waves become narrower and agree better with theory. These findings are in agreement with our previous work for K-I [20].

4.2.3. The model ionophore Li-VI

The lithium ionophore Li-VI incorporating a 14-crown-4 unit was reported as the most selective crown ether derivative for the recognition of lithium. It is believed to force 1:1 complexes by a steric suppression of 1:2 sandwich-type complexes with potassium and sodium, which helps to improve selectivity over these two monovalent ions [28,29]. The best fits from three replicates give $\log \beta_{LiL} = 4.31 \pm 0.04$, and this requires an ionophore concentration of 5.97 ± 1.11 mmol/kg, which is about half the experimental concentration but this value agrees with the literature, $\log \beta_{LiL} = 4.37 \pm 0.01$ [22]. However, the quality of the theoretical fit can be improved if the stoichiometric binding ratio is changed to 1:2 with an ionophore concentration of 13.77 ± 1.53 mmol/kg (seen in Fig. 4c), which gives $\log \beta_{LiL2} = 5.97 \pm 0.06$. The comparison of the two fits is shown in Fig. S7 (see Supplementary Information). The formation of 1:2 complexes with lithium seems implausible given the expected steric hindrance of such a structure, but the need for half the experimental concentration for an agreement with the data is equally uncomfortable. The question of accurate stoichiometry is therefore not clearly resolved by the available data.

The formation constants obtained for the other ions with Li-VI are $\log \beta_{KL} = 2.48 \pm 0.03$, $\log \beta_{NaL2} = 4.57 \pm 0.21$ (stoichiometric ratio of 1:2), $\log \beta_{CaL} = 0.47 \pm 0.03$, $\log \beta_{MgL3} = 8.08 \pm 0.03$ (stoichiometric ratio of 1:3). The corresponding selectivity coefficients were calculated as $\log K_{Li,K}^{pot} = -0.78 \pm 0.17$, $\log K_{Li,Na}^{pot} = -1.22 \pm 0.54$, which compare only moderately to the literature values of -1.9 and -1.9. However, the observed values for the divalent ions are $\log K_{Li,Mg}^{pot} = -2.75 \pm 0.15$ and $\log K_{Li,Ca}^{pot} = -3.80 \pm 0.15$ that are closer to the reported ones of -4.6 and -4.4 [30]. The peak separation for the membrane containing Li-VI decreases similarly to Na-X when comparing to the uncorrected data without subtracting the POT potential change (Fig. 4d).

4.2.4. The model ionophore Ca-IV

The noncyclic calcium ionophore ETH 5234 containing diamides and ether oxygen groups possesses a high affinity to calcium, known to form a 1:3 complex [31]. The observed formation constant $\log \beta_{CaL3} = 21.57 \pm 0.25$ (stoichiometric ratio of 1:3) obtained from the data in Fig. 4e is indeed very close to the literature value $\log \beta_{CaL3} = 22.06 \pm 0.08$ [22]. Note that the data shown gives no evidence for a stepwise decomplexation upon increasing ion-exchanger concentration, so 1:3 complexes may be regarded as the only possible stoichiometry. Consequently, Ca-IV demonstrates an outstanding selectivity over all other ions as shown in Fig. 4e. The data is compatible with 1:1 complex with the studied monovalent ions, which translates into the binding constants of $\log \beta_{KL} = 3.97 \pm 0.06$, $\log \beta_{NaL} = 4.84 \pm 0.05$, and $\log \beta_{LiL} = 4.27 \pm 0.06$. On the other hand, the data suggest concurrent 1:1 and 1:3 complexes with magnesium with $\log \beta_{MgL} = 5.53 \pm 0.05$ and $\log \beta_{MgL3} = 12.23 \pm 0.75$. By considering these multiple ion-ionophore complex stoichiometries coexisting in the membrane, we may visualize how the selectivity coefficient changes with different R_T / L_T ratios. This results in a lower selectivity for Ca-IV over magnesium than if one considers exclusively 1:1 or 1:3 ion-ionophore complex in the membrane. Experimentally, a selectivity coefficient $\log K_{Ca,Mg}^{pot} = -14.36 \pm 1.63$ is observed. A twelve orders of magnitude discrimination of magnesium is outstanding and is fall just short of the minimum possible value for the complete absence of magnesium complexation, calculated as -16.7 [22]. The experimental selectivity coefficients over potassium, sodium and lithium are $\log K_{Ca,K}^{pot} = -7.94 \pm 0.20$, $\log K_{Ca,Na}^{pot} = -9.85 \pm 0.15$ and $\log K_{Ca,Li}^{pot} = -10.13 \pm 0.30$. Comparing to the available literature data with a different plasticizer (NPOE), $\log K_{Ca,K}^{pot} = -9.6$, $\log K_{Ca,Na}^{pot} = -7.9$, $\log K_{Ca,Li}^{pot} = -7.7$ and $\log K_{Ca,Mg}^{pot} = -8.9$ [16], the selectivity coefficients of Ca-IV over different ions are different, likely because of the different matrix. These extremely high selectivity coefficients reflect the weak binding of these ions with Ca-IV as evidenced in Fig. 4e. We note, however, that the thin layer technique proposed here suggests even higher selectivity. This may be explained with the exhaustive expulsion of the relevant cations from the membrane at the end of each anodic scan that results in a mass transport limited uptake of dilute interferences during each cathodic scan [32], which should reduce the undesired bias originating from calcium impurities contained in each electrolyte. Similar to the other ionophores discussed above, the two ion transfer peaks become closer than with the uncorrected data, see Fig. 4f. For all ionophores, the ion transfer waves after subtracting the contribution from POT give a good agreement with literature data.

The observed formation constants for each ionophore toward different ions are summarized in Table 1. Complete data postprocessing and the best theoretical fit from three replicates for membranes MIV, MV and MVII containing Na-X, Li-VI and Ca-IV respectively are shown in Fig. S5. As expected, each membrane reverts to the Hofmeister sequence when increasing ion-exchanger concentration beyond saturation of ionophore (right most data in Figs. 4a, 4c,4e). In those cases, the potentials of the ions follow the trend potassium > sodium > lithium > calcium > magnesium, as established. Decreasing the concentration of ion exchanger gives partial complexation of the ionophore and results in a dramatic increase in potential since almost all ions bind with the ionophore. Within this range one can normally find the optimum composition for best membrane selectivity.

Some uncertainty in the measurements involving magnesium salts is noted where the potentials are found to be higher than theoretical expectations at low concentrations of ion exchanger. This is especially

relevant for the membrane containing Ca-IV. This may be caused by interfering ions (specifically calcium impurities) in the magnesium salt. Bühlmann's group recently reported on the difficulty of observing multiple simultaneous complex stoichiometries with ion-selective membranes [33,34]. An interfering ion complex of a different stoichiometry simultaneously present in the membrane may indeed strongly influence the apparent selectivity at a very low concentration of ion exchanger [7].

For the 1:3 ratio of the calcium-Ca-IV complex, it is possible that the complexation/decomplexation kinetics are not sufficiently rapid for a strict thermodynamic treatment, as suggested by the group of Amemiya [35]. This might also be the reason for the imperfect fit of the potential inflection in Fig. 4c and for the larger resulting standard deviations for this ionophore. On the other hand, the correspondence of the binding constants with literature data is encouraging. The possible limitation of binding kinetics on this type of experiments merits a more detailed future investigation that goes beyond the scope of this work.

4.2.5. *Non-ionic surfactants*

Surfactants are amphiphilic compounds that reduce the surface tension between two immiscible phases. Many non-ionic surfactants that possess polyethylene oxide as the hydrophilic moiety, like Brij-35, F127 and TX-100 studied here, have shown strong binding constants with cations in an organic phase [5]. Potentiometric measurements may also provide binding constants of surfactants, but those experiments are limited to a discrete ion-exchanger concentration [36,37]. In addition, as Fig. S9 shows, this binding phenomenon during thin film ion transfer voltammetry contradicts the results expected from simple surfactant partitioning. Specifically, a surfactant bulk concentration change of an order of magnitude (still below the surfactant CMC) does not shift the ion-surfactant complex peak potential in accordance to the Nernst equation. Instead, the peak current increases as more surfactant is added into the bulk solution. This implies that surfactants accumulate at the membrane interface resulting in a local concentration significantly greater than in solution. Although not entirely surprising due to the nature of surfactants, this potentially saturated interface has implications for our analysis. Eq. 9 is no longer applicable and the term for the concentration of surfactant in the membrane ($c_M^m P_s$) for Eq. 12 is defined as a constant estimated by the height of the surfactant associated peak.

Following theoretical fitting using Eqs. (8) and (12) we again obtained the best fit using 1:1 ion-valinomycin complexation and found that all surfactants also seem to undergo 1:1 complexation shown in Fig. 5 (membrane composition is VIII as in Table. S1). To obtain a more stable formal potential of the ion transfer in solution with surfactant, POT was replaced with the more lipophilic transducer, PEDOT-C_{14}. Based on the optimal fit, binding constants of each surfactant with potassium ion were found to be as follows, log $\beta_{KBrij\text{-}35} = 4.88 \pm 0.08$, log $\beta_{KF127} = 4.63 \pm 0.49$, log $\beta_{KTX\text{-}100} = 5.63 \pm 0.10$. The binding constant for the ion-valinomycin complex (the same as indicated in Section 4.2.1) can be used as a reference point for comparison against for ion-surfactant binding, which is around five orders of magnitude less. Therefore, the potential difference between ionophore and surfactant complexes can also be estimated by the binding constant and this increases reliability when fitting the theoretical curve with experimental data (data postprocessing details shown in Fig. S8). The fits obtained here provide strong evidence to support the hypothesis formed in our previous work [5] i.e. that all three non-ionic surfactants here form 1:1 complexes with potassium ions. Fits obtained using other

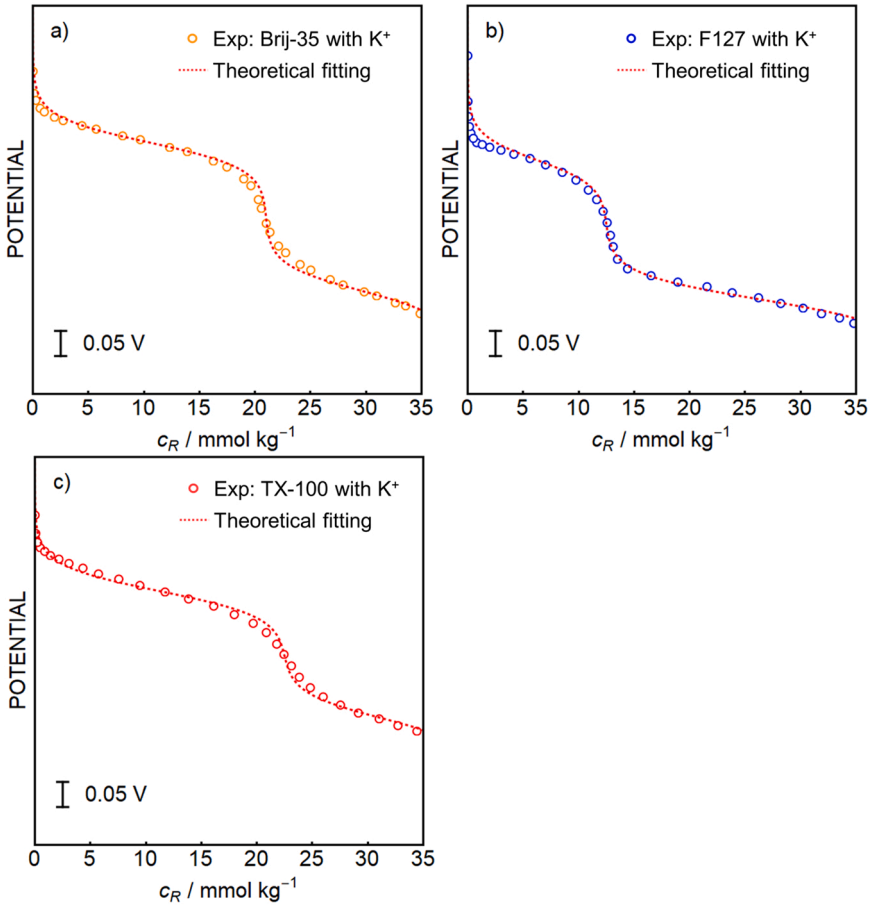

Fig. 5. Theoretical fitting of ion transfer curves for different surfactants using equilibrium theory and comparison with the experimental data, a) Brij-35, b) F127 and c) TX-100 performed in solution containing 10 mM KCl, respectively.

stoichiometries of TX-100:K^+ (1:2 and 1:3) show extreme deviations from the experimental data, as shown in Fig. S9.

4.3. Application to polyurethane membranes

The approach was also explored using a second polymeric matrix substrate, plasticized polyurethane (PU), which has demonstrated improved robustness compared to the valinomycin containing PVC studied above [38]. The phase boundary potential change was extracted by the same procedure (details in Fig. S6). Smaller values were obtained for the formation constants of valinomycin with potassium and sodium, $\log\beta_{KL} = 8.07 \pm 0.05$ and $\log\beta_{NaL} = 3.53 \pm 0.17$. These values were cross validated with the potentiometric sandwich membrane method (see SI, Experimental procedures), giving $\log\beta_{KL} = 7.94 \pm 0.22$ and $\log\beta_{NaL} = 3.45 \pm 0.35$. The decrease in formation constants is understood to be the result of coordinating functional groups in polyurethane that may partially solvate uncomplexed ions.

5. Conclusions

In summary, the thin layer ion transfer voltammetric approach studied here is extremely useful for the characterization of ion-ionophore interactions. We were able to obtain insights on complexation stoichiometry and measure ionophore complex formation constants in ion-selective membranes. Using the same data set it was also possible to extract selectivity coefficients for a continuously varying membrane composition. For reliable comparison with other literature sources, this study chose PVC/DOS as the primary matrix substrate because of its widespread use. The formation constants of K-I, Na-X, Ca-IV obtained here are very close to literature data, while for Li-VI, the best fit suggests the formation of 1:2 complexes, which was unexpected. The approach has potential for careful assessment of ion-ionophore binding stoichiometry and formation constants in the membrane under thermodynamic conditions. The selectivity coefficients calculated from this method agree in most cases with the data from the literature, typically taken from the common optimum membrane composition ($R_T / L_T < 1$). It may also give experimental information about the optimum selectivity as a function of different R_T / L_T ratios that helps one to adjust the membrane composition effectively. The thin layer membrane configuration helps to minimize mass transport limitations, which largely simplifies mathematical treatment and reduces experimental bias. Some potential limitations of the approach are noted. It requires materials of sufficient lipophilicity and stability for a successful experiment. The ions of interest should not exhibit a chemical affinity to the underlying transducing material. For example, anions may interact electrostatically with cationic oxidized POT and have been shown experimentally to negatively impact polymer stability [19]. One should experimentally confirm the absence of chemical interaction between ionophore and the selected reference ion. If ion pairing is important, the theoretical model should incorporate this effect, as well as the coexistence of multiple stoichiometries. The voltammetric signal may be kinetically limited by the ion–ionophore recognition as well, in which case the model should be adapted accordingly [35,39].

CRediT authorship contribution statement

Canwei Mao: Conceptualization, Methodology, Validation, Formal analysis, Investigation, Writing – original draft, Visualization. **Kye Robinson:** Conceptualization, Investigation, Writing – review & editing. **Dajing Yuan:** Conceptualization, Methodology, Writing – original draft. **Eric Bakker:** Conceptualization, Methodology, Writing – review & editing, Supervision.

Declaration of Competing Interest

The authors declare that they have no known competing financial interests or personal relationships that could have appeared to influence the work reported in this paper.

Acknowledgment

The C.M., K.R. and E.B. thank the Swiss National Science Foundation (SNSF) for financial support of this work and Y.D. acknowledges the support from the Natural Science Foundation of Anhui Province (2108085QB67).

Appendix A. Supporting information

Supplementary data associated with this article can be found in the online version at doi:10.1016/j.snb.2022.131428.

References

[1] C. Bieg, K. Fuchsberger, M. Stelzle, Introduction to polymer-based solid-contact ion-selective electrodes—basic concepts, practical considerations, and current research topics, Anal. Bioanal. Chem. 409 (2017) 45–61, https://doi.org/10.1007/s00216-016-9945-6.
[2] E. Bakker, P. Bühlmann, E. Pretsch, Carrier-Based Ion-Selective Electrodes and Bulk Optodes. 1. General Characteristics, Chem. Rev. 97 (1997) 3083–3132, https://doi.org/10.1021/cr940394a.
[3] E. Malinowska, M.E. Meyerhoff, Influence of nonionic surfactants on the potentiometric response of ion-selective polymeric membrane electrodes designed for blood electrolyte measurements, Anal. Chem. 70 (1998) 1477–1488, https://doi.org/10.1021/ac970761t.
[4] C. Burger-Guerrisi, C. Tondre, Conductometric study of the interaction of 1:1 electrolytes with nonionic surfactants having short polyoxyethylated chains: methanolic solutions of H- and F-alkylated surfactants and oil/water microemulsions, J. Colloid Interface Sci. 116 (1987) 100–108, https://doi.org/10.1016/0021-9797(87)90102-0.
[5] K. Robinson, C. Mao, E. Bakker, Surfactants for optode emulsion stabilization without sacrificing selectivity or binding constants, Anal. Chem. 93 (2021) 15941–15948, https://doi.org/10.1021/acs.analchem.1c03232.
[6] R.D. Johnson, L.G. Bachas, Ionophore-based ion-selective potentiometric and optical sensors, Anal. Bioanal. Chem. 376 (2003) 328–341, https://doi.org/10.1007/s00216-003-1931-0.
[7] I. Yilmaz, L.D. Chen, X.V. Chen, E.L. Anderson, R.C. da Costa, J.A. Gladysz, P. Bühlmann, Potentiometric selectivities of ionophore-doped ion-selective membranes: concurrent presence of primary ion or interfering ion complexes of multiple stoichiometries, Anal. Chem. 91 (2019) 2409–2417, https://doi.org/10.1021/acs.analchem.8b05196.
[8] P.C. Meier, W.E. Morf, M. Läubli, W. Simon, Evaluation of the optimum composition of neutral-carrier membrane electrodes with incorporated cation-exchanger sites, Anal. Chim. Acta 156 (1984) 1–8, https://doi.org/10.1016/S0003-2670(00)85531-2.
[9] R. Eugster, P.M. Gehrig, W.E. Morf, U.E. Spichiger, W. Simon, Selectivity-modifying influence of anionic sites in neutral-carrier-based membrane electrodes, Anal. Chem. 63 (1991) 2285–2289, https://doi.org/10.1021/ac00020a017.
[10] V.A. Nazarov, K.A. Andronchik, V.V. Egorov, V.E. Matulis, O.A. Ivashkevich, Intramembrane complex formation study of ion selective electrodes based on heptyl p-trifluoroacetylbenzoic ether, Electroanalysis 23 (2011) 1058–1066, https://doi.org/10.1002/elan.201000606.
[11] M.M. Shultz, O.K. Stefanova, S.B. Mokrov, K.N. Mikhelson, Potentiometric estimation of the stability constants of ion−ionophore complexes in ion-selective membranes by the sandwich membrane method: theory, advantages, and limitations, Anal. Chem. 74 (2002) 510–517, https://doi.org/10.1021/ac015564f.
[12] P.J. Greenawalt, M.B. Garada, S. Amemiya, Voltammetric characterization of ion–ionophore complexation using thin polymeric membranes: asymmetric thin-layer responses, Anal. Chem. 87 (2015) 8564–8572, https://doi.org/10.1021/acs.analchem.5b02355.
[13] Y. Mi, E. Bakker, Determination of complex formation constants of lipophilic neutral ionophores in solvent polymeric membranes with segmented sandwich membranes, Anal. Chem. 71 (1999) 5279–5287.
[14] Á. Molina, J.A. Ortuño, C. Serna, E. Torralba, Physical insights of salt transfer through solvent polymeric membranes by means of electrochemical methods, Phys. Chem. Chem. Phys. 12 (2010) 13296, https://doi.org/10.1039/c0cp00272k.
[15] S.M. Ulmeanu, H. Jensen, Z. Samec, G. Bouchard, P.-A. Carrupt, H.H. Girault, Cyclic voltammetry of highly hydrophilic ions at a supported liquid membrane, J. Electroanal. Chem. 530 (2002) 10–15, https://doi.org/10.1016/S0022-0728(02)01002-1.
[16] H. Perera, A. Shvarev, Determination of unbiased selectivity coefficients using pulsed chronopotentiometric polymeric membrane ion sensors, Anal. Chem. 80 (2008) 7870–7875, https://doi.org/10.1021/ac801210u.
[17] Y. Liu, G.A. Crespo, M. Cuartero, Semi-empirical treatment of ionophore-assisted ion-transfers in ultrathin membranes coupled to a redox conducting polymer, Electrochim. Acta 388 (2021), 138634, https://doi.org/10.1016/j.electacta.2021.138634.

[18] E. Laborda, J. González, A. Molina, Analytical theory for ion transfer–electron transfer coupled reactions at redox layer–modified/thick film–modified electrodes, Curr. Opin. Electrochem. 19 (2020) 78–87, https://doi.org/10.1016/j.coelec.2019.10.007.
[19] D. Yuan, M. Cuartero, G.A. Crespo, E. Bakker, Voltammetric thin-layer ionophore-based films: part 1. Experimental evidence and numerical simulations, Anal. Chem. 89 (2017) 586–594, https://doi.org/10.1021/acs.analchem.6b03354.
[20] C. Mao, D. Yuan, L. Wang, E. Bakker, Separating boundary potential changes at thin solid contact ion transfer voltammetric membrane electrodes, J. Electroanal. Chem. 880 (2021), 114800, https://doi.org/10.1016/j.jelechem.2020.114800.
[21] E. Bakker, Determination of improved selectivity coefficients of polymer membrane ion-selective electrodes by conditioning with a discriminated ion, J. Electrochem. Soc. 143 (1996) L83–L85, https://doi.org/10.1149/1.1836608.
[22] Y. Qin, Y. Mi, E. Bakker, Determination of complex formation constants of 18 neutral alkali and alkaline earth metal ionophores in poly(vinyl chloride) sensing membranes plasticized with bis(2-ethylhexyl)sebacate and o-nitrophenyloctylether, Anal. Chim. Acta 421 (2000) 207–220, https://doi.org/10.1016/S0003-2670(00)01038-2.
[23] E. Bakker, E. Pretsch, P. Bühlmann, Selectivity of potentiometric ion sensors, Anal. Chem. 72 (2000) 1127–1133, https://doi.org/10.1021/ac991146n.
[24] T. Grady, A. Cadogan, T. McKittrick, S.J. Harris, D. Diamond, M.A. McKervey, Sodium-selective electrodes based on triester monoacid derivatives of p-tert-butylcalix[4]arene. Comparison with tetraester calix[4]arene ionophores, Anal. Chim. Acta 336 (1996) 1–12, https://doi.org/10.1016/S0003-2670(96)00380-7.
[25] A.M. Cadogan, D. Diamond, M.R. Smyth, M. Deasy, M.A. McKervey, S.J. Harris, Sodium-selective polymeric membrane electrodes based on calix[4]arene ionophores, Analyst 114 (1989) 1551, https://doi.org/10.1039/an9891401551.
[26] K. Kimura, T. Matsuba, Y. Tsujimura, M. Yokoyama, Unsymmetrical calix[4]arene ionophore/silicone rubber composite membranes for high-performance sodium ion-sensitive field-effect transistors, Anal. Chem. 64 (1992) 2508–2511, https://doi.org/10.1021/ac00045a009.
[27] X. Yang, Development of a fluorescent optode membrane for sodium ion based on the calix[4]arene and tetraphenylporphine, Talanta 52 (2000) 1033–1039, https://doi.org/10.1016/S0039-9140(00)00469-0.
[28] S. Kitazawa, K. Kimura, H. Yano, T. Shono, Lipophilic crown-4 derivatives as lithium ionophores, J. Am. Chem. Soc. 106 (1984) 6978–6983, https://doi.org/10.1021/ja00335a019.
[29] K. Kimura, H. Yano, S. Kitazawa, T. Shono, Synthesis and selectivity for lithium of lipophilic 14-crown-4 derivatives bearing bulky substituents or an additional binding site in the side arm, J. Chem. Soc. Perkin Trans. 2 (1986) 1945, https://doi.org/10.1039/p29860001945.
[30] K. Kimura, H. Oishi, T. Miura, T. Shono, Lithium ion selective electrodes based on crown ethers for serum lithium assay, Anal. Chem. 59 (1987) 2331–2334, https://doi.org/10.1021/ac00146a004.
[31] E. Pretsch, D. Ammann, H.F. Osswald, M. Güggi, W. Simon, Ionophore vom Typ der 3-Oxapentandiamide, Helv. Chim. Acta 63 (1980) 191–196, https://doi.org/10.1002/hlca.19800630117.
[32] D. Yuan, E. Bakker, Overcoming pitfalls in boundary elements calculations with computer simulations of ion selective membrane electrodes, Anal. Chem. 89 (2017) 7828–7831, https://doi.org/10.1021/acs.analchem.7b01777.
[33] R. Eugster, U.E. Spichiger, W. Simon, Membrane model for neutral-carrier-based membrane electrodes containing ionic sites, Anal. Chem. 65 (1993) 689–695, https://doi.org/10.1021/ac00054a007.
[34] M. Miyake, L.D. Chen, G. Pozzi, P. Bühlmann, Ion-selective electrodes with unusual response functions: simultaneous formation of ionophore–primary ion complexes with different stoichiometries, Anal. Chem. 84 (2012) 1104–1111, https://doi.org/10.1021/ac202761x.
[35] S. Amemiya, Voltammetric ion selectivity of thin ionophore-based polymeric membranes: kinetic effect of ion hydrophilicity, Anal. Chem. 88 (2016) 8893–8901, https://doi.org/10.1021/acs.analchem.6b02551.
[36] C. Espadas-Torre, E. Bakker, S. Barker, M.E. Meyerhoff, Influence of nonionic surfactants on the potentiometric response of hydrogen ion-selective polymeric membrane electrodes, Anal. Chem. 68 (1996) 1623–1631, https://doi.org/10.1021/ac951017g.
[37] K.N. Mikhelson, Ion-Selective Electrodes, Springer Berlin Heidelberg, Berlin, Heidelberg, 2013, https://doi.org/10.1007/978-3-642-36886-8.
[38] M. Cuartero, G.A. Crespo, E. Bakker, Polyurethane ionophore-based thin layer membranes for voltammetric ion activity sensing, Anal. Chem. 88 (2016) 5649–5654, https://doi.org/10.1021/acs.analchem.6b01085.
[39] R. Ishimatsu, A. Izadyar, B. Kabagambe, Y. Kim, J. Kim, S. Amemiya, Electrochemical mechanism of ion–ionophore recognition at plasticized polymer membrane/water interfaces, J. Am. Chem. Soc. 133 (2011) 16300–16308, https://doi.org/10.1021/ja207297q.

Mr. Canwei Mao is a doctoral student in the group of Prof. Eric Bakker at the University of Geneva. His research interests are in fundamental aspects of ion sensing, with a particular focus on thin membrane ion transfer voltammetric principles, the interaction of neutral surfactants with ion-selective membranes, the design of ion-transfer voltammetric microelectrodes and the uptake processes of emulsified nanosensors by ion-selective membranes.

Dr. Kye Robinson obtained his BSc (Hons) in chemistry at the University of Queensland in 2014 before moving to Monash University to complete his Ph.D. under the supervision of Dr. Simon Corrie in 2019. Following his Ph.D. he was awarded a Swiss Postdoctoral Scholarship to carry out research under the supervision of Prof. Eric Bakker at the university of Geneva where he is continuing as a postdoctoral researcher developing new mechanisms for and improving the performance of optical ion sensors.

Dr. Dajing Yuan obtained his Ph.D. at the University of Geneva, working on the topic of thin membrane ion transfer voltammetric principles, solid contact ion-selective electrodes and improved theoretical models to describe ion fluxes at ion-selective membranes. He is currently an assistant professor at Anhui University in China.

Dr. Eric Bakker is professor of Analytical Chemistry at the University of Geneva. He received his Ph.D. from ETH Zurich and spent 14 years in the U.S. as faculty member at Auburn University and Purdue University as well as three years in Australia at Curtin University before moving to Geneva in 2010. His interests are in chemical sensors, with a particular emphasis on ion-selective membranes. He has published more than 350 papers so far.